Transactions of the Materials Research Society of Japan 30[1] 299-302 (2005)

Absolute densities of Ti atoms and Ti^+ ions in magnetron sputtering plasmas measured by laser-induced fluorescence

N. Nafarizal, N. Takada, K. Nakamura[1)], T.Yoshida[2)] and K. Sasaki
Department of Electrical Engineering and Computer Science, Nagoya University, Nagoya 464-8603
[1)]Department of Electrical Engineering, Chubu University, Kasugai 487-8501
[2)]Electron Device Equipment, Engineering Div., ANELVA Corporation, Fuchu 183-8508
Fax: 81-052-788-6603, e-mail: n_nayan@echo.nuee.nagoya-u.ac.jp

We measured the spatial distributions of Ti and Ti^+ densities in magnetron sputtering plasmas. The ground states of Ti (a^3F_J) and Ti^+ (a^4F_J) consist of several sublevels with different J numbers. We evaluated the total Ti and Ti^+ densities by determining the densities of the sublevels separately. The measurements of two-dimensional distributions of relative densities were done by laser-induced fluorescence imaging spectroscopy. The absolute local densities were determined by comparing the relative density distributions with the line-integrated absolute densities measured by optical absorption spectroscopy using a hollow cathode Ti lamp as a light source. As a result, the Ti density at the peak position was approximately 4.6×10^{11} cm^{-3} at a dc discharge power of 75 W and an Ar gas pressure of 100 mTorr. On the other hand, the Ti^+ density at the peak position was approximately 1.5×10^{10} cm^{-3} at the same discharge condition.

Key words: Titanium atom, Titanium ion, Absolute density, Magnetron sputtering, LIF

1. INTRODUCTION

Magnetron sputtering plasmas are widely used as efficient tools for thin film deposition. At present, in the interconnection wiring process by the damascene method in the fabrication of ultra-large scale integrated circuits (ULSI), magnetron sputtering is used for the deposition of barrier and seed layers in trenches and holes. In this process, the ratio of metal ion to atom densities is important since a high ion concentration is utilized to obtain directional deposition in narrow trenches and holes. Several simulations and experiments have been carried out to study the spatial density distributions of atoms and ions in magnetron sputtering plasmas [1-3].

In the present work, we measured the spatial distributions of Ti and Ti^+ densities experimentally by laser-induced fluorescence (LIF) imaging spectroscopy combined with ultraviolet absorption spectroscopy (UVAS). Ti is generally used as a barrier metal against Al wiring in ULSI. Since the ground states of Ti and Ti^+ are composed of several sublevels, the densities of the sublevels were evaluated separately. The total densities of Ti and Ti^+ were obtained by summing the densities of the sublevels.

2. EXPERIMENTAL SETUP

2.1 Magnetron sputtering

Figure 1 shows the experimental setup for the two-dimensional LIF measurement. A magnetron sputtering source was inserted from the top of a vacuum chamber. The magnetron source was a conventional type with cylindrical permanent magnets on an indirect water-cooling system. The maximum magnetic field of

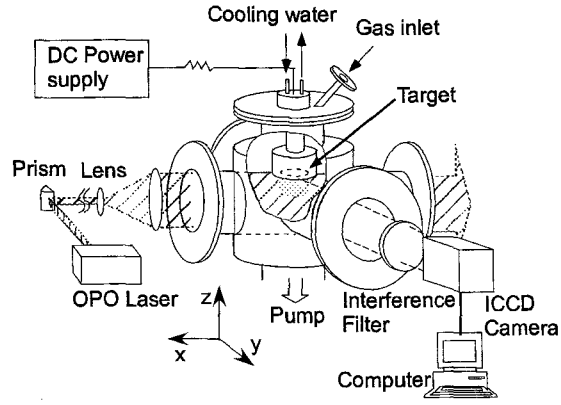

Figure 1. Experimental setup for two-dimensional laser-induced fluorescence measurement.

the permanent magnets was 1.2 kG on the target surface. Base pressure of the vacuum chamber was approximately 10^{-7} Torr, which was obtained by evacuating the chamber using the combination of a turbomolecular pump and an oil rotary pump. Sputtering plasmas were produced by direct-current (dc) magnetron discharges with a Ti target of 50 mm in diameter. The discharge gas was Ar and the pressure was measured using a capacitance manomator.

2.2 Laser-induced fluorescence imaging spectroscopy

The two-dimensional distributions of the Ti and Ti^+ densities in the magnetron sputtering plasma source were measured by LIF imaging spectroscopy. Tunable laser pulses yielded from an optical parametric oscillator (OPO) were injected into plasmas in front of the Ti

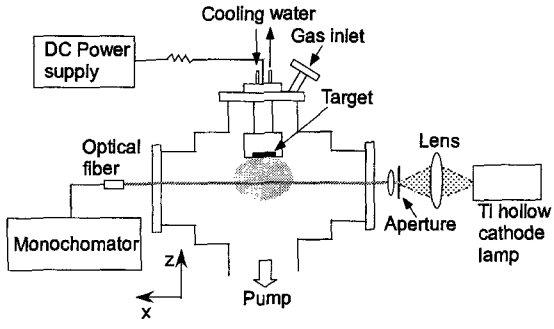

Figure 2. Experimental setup for ultraviolet absorption spectroscopy.

target. The tunable laser beam was arranged to have a planar shape by using two cylindrical lenses. The width and the thickness of the planar laser beam were 80 and 2 mm, respectively. The wavelengths of the OPO laser were tuned to excite Ti and Ti^+ in plasmas. Excited Ti and Ti^+ yielded fluorescences on the planar OPO laser beam. The pictures of the fluorescence images were taken by a gated charge-coupled device (CCD) camera with an image intensifier. Interference filters were placed to separate the fluorescences from the stray lights and self-emissions from plasmas. In this way, the two-dimensional distributions of the Ti and Ti^+ densities in plasmas were obtained. Since the ground states of Ti (a^3F_J) and Ti^+ (a^4F_J) are composed of three and four sublevels, respectively, we measured the densities of the sublevels separately. The energy levels and wavelengths used in the present LIF imaging spectroscopy are summarized in Table I.

Table I. Energy levels and wavelengths used in LIF imaging spectroscopy [4,5].

	Initial state	Excitation wavelength	Excited state	Fluore-scence	Final state
Ti	a^3F_2	293.352nm	$v^3F^o_3$	445.532nm	b^3F_3
Ti	a^3F_3	294.838nm	$v^3F^o_3$	445.532nm	b^3F_3
Ti	a^3F_4	295.618nm	$v^3F^o_4$	445.743nm	b^3F_4
Ti^+	$a^4F_{3/2}$	324.198nm	$z^4F^o_{3/2}$	334.034nm	$b^4F^o_{3/2}$
Ti^+	$a^4F_{5/2}$	323.904nm	$z^4F^o_{5/2}$	334.672nm	$b^4F^o_{7/2}$
Ti^+	$a^4F_{7/2}$	323.657nm	$z^4F^o_{7/2}$	334.377nm	$b^4F^o_{9/2}$
Ti^+	$a^4F_{9/2}$	323.452nm	$z^4F^o_{9/2}$	334.294nm	$b^4F^o_{9/2}$

2.3 Ultraviolet absorption spectroscopy

The density distributions of Ti and Ti^+ obtained by the LIF measurements do not provide us with the absolute densities. We carried out UVAS to determine the absolute densities of Ti and Ti^+. Figure 2 shows the experimental setup for the UVAS measurement. The light from a hollow cathode Ti lamp was arranged to be a collimated beam and was launched into plasmas. The emission transmitted through the plasma was detected using a mutlichannel detector via a monochoromator.

The absorption transitions of Ti from the sublevels are at 363.55 nm ($a^3F_2 \rightarrow y^3G^o_3$), 364.27 nm ($a^3F_3 \rightarrow y^3G^o_4$), and 365.35 nm ($a^3F_4 \rightarrow y^3G^o_5$). A conventional theory was adopted to evaluate the absolute line-integrated density from absorption [6]. The local Ti density was determined by comparing the

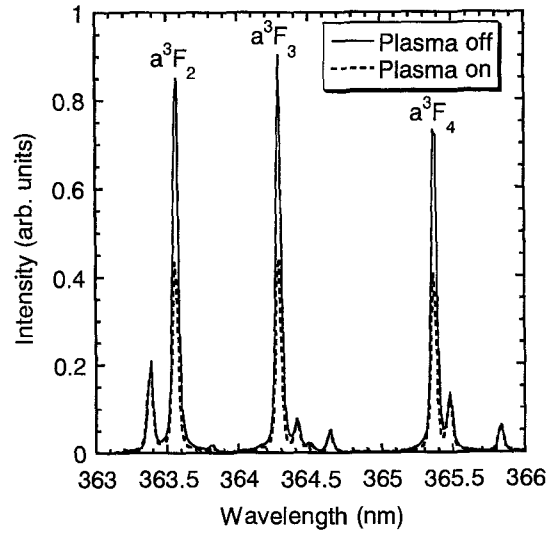

Figure 3. Emission spectrum from a hollow cathode Ti lamp.

line-integrated absolute density with the distribution of the relative Ti density measured by LIF imaging spectroscopy. Although we also tried to detect emissions of Ti^+ to the sublevels, we detected the emission only at 323.66 nm ($a^4F_{7/2} \leftarrow z^4F^o_{7/2}$) because of the weak intensity of the hollow cathode lamp. Hence the densities of the sublevels of Ti^+ (a^4F_J) other than J=7/2 were estimated by considering the transition probabilities of the transitions employed in the LIF measurement.

3. RESULTS AND DISCUSSION

3.1 Absolute densities of Ti (a^3F_J) atoms

Figure 3 shows the emission spectrum from the hollow cathode lamp in the wavelength range from 363 to 366 nm. The distance between the target surface and the collimated lamp beam was 3.5 cm, and the plasma was produced at a discharge power of 75 W and an Ar gas pressure of 100 mTorr. The emissions indicated by a^3F_J (J=2,3,4) are the resonant transitions of Ti. It is clearly shown in the figure that the intensities of the resonant transitions transmitted through the plasma are weaker than those without the plasma, while the intensities of the other emissions are not weakened by the plasma. The line-integrated densities of the sublevels were calculated from the absorptions, by assuming a temperature of 300 K for Ti atoms in the plasma. This assumption may be reasonable since the measurement is carried out in the downstream plasma with a distance of 3.5 cm from the target.

In order to evaluate the local absolute Ti density, the line-integrated density measured by UVAS was compared with the distribution of the relative density measured by LIF. The distribution of the Ti density measured by LIF was integrated numerically along the measurement chord of UVAS. The comparisons between the absolute line densities and the relative line densities for the sublevels are plotted in Fig. 5. As shown in the figure, proportional relationships were found between the absolute line densities and the

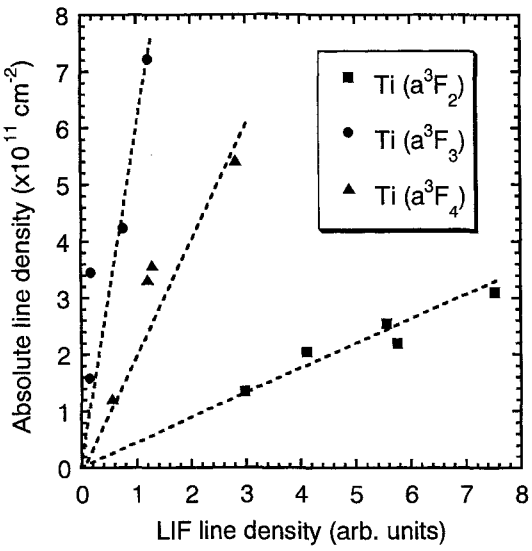

Figure 5. Comparison between the absolute line densities and relative line densities for Ti (a^3F_J).

relative line densities. The distributions of the relative Ti densities obtained by LIF were thus calibrated, and the local absolute densities of the sublevels were evaluated.

Figure 6 shows the two-dimensional distributions of the absolute Ti densities of the sublevels. The discharge power and the Ar gas pressure were 75 W and 100 mTorr, respectively. The shapes of the density distributions of the sublevels were almost the same. The absolute densities at r=0 cm and z=1 cm (r and z stand for the radial position and the distance from the target, respectively), which corresponded to the peak position in the density distributions, were 3.5x10^{11} cm^{-3} for a^3F_2, 1.2x10^{11} cm^{-3} for a^3F_3, and 9.1x10^{10} cm^{-3} for a^3F_4. Hence the total absolute density was evaluated to be 4.6x10^{11} cm^{-3}. The population ratio of the sublevels was a^3F_2: a^3F_3: a^3F_4=1.0:0.35:0.26.

A temperature can be evaluated by plotting the population ratio with respect to their energies. The population ratios were roughly approximated by Boltzmann distributions. Figure 7 shows one-dimensional distribution of the temperature along the symmetric axis, together with the densities of the sublevels and the total Ti atom density. The origin of the horizontal axis corresponds to the target surface. The Ti atom density decreased exponentially with the distance from the target, while the temperature was roughly constant at 320 K in the entire discharge space.

3.2 Absolute densities of Ti$^+$ (a^4F_J) ions

As mentioned above, the emissions of Ti$^+$ from the hollow cathode lamp was weak, so that the emission intensities corresponding to the transitions to the a^4F_J states with J=3/2, 5/2, and 9/2 were below the detection limit. We detected the emission only at 323.66 nm corresponding to the transition of $a^4F_{7/2}$←$z^4F^o_{7/2}$, and we determined the absolute density of Ti$^+$ at the $a^4F_{7/2}$ state. The comparison between the absolute line density measured by UVAS and the relative line density obtained by LIF is shown in Fig. 8. The local absolute density of the $a^4F_{7/2}$ state was evaluated from the proportional relationship. On the other hand, the LIF

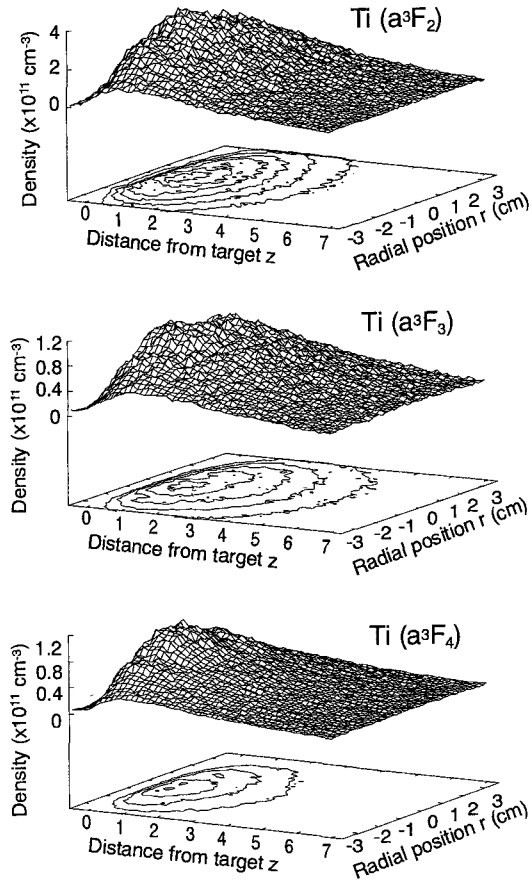

Figure 6. Two-dimensional distributions of the Ti(a^3F_J) densities. The discharge power was 75 W and the Ar gas pressure was 100 mTorr.

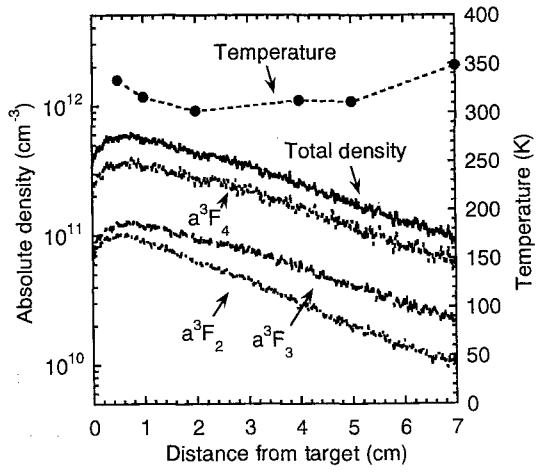

Figure 7. One-dimensional distributions of the Ti (a^3F_J) densities, the total Ti atom density, and the temperature evaluated from the population ratio. The discharge power was 75 W and the Ar gas pressure was 100 mTorr.

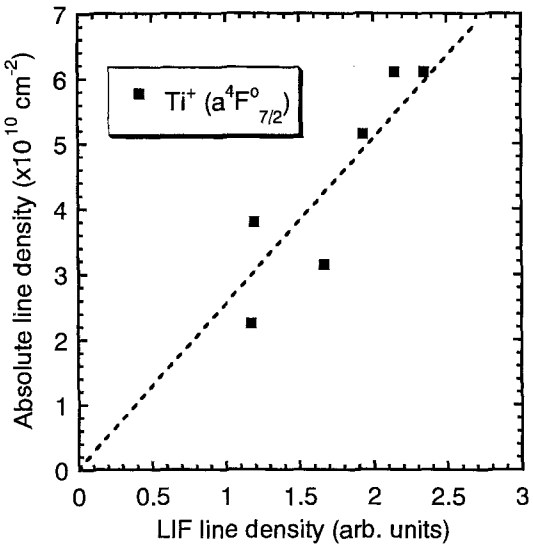

Figure 8. Comparison between the absolute line density and the relative line density for Ti^+ ($a^4F_{7/2}$).

measurement was so sensitive that we detected the distributions of the densities of the a^4F_J states with J=3/2, 5/2, and 9/2. Since sufficient saturation is expected for the excitation transitions of LIF because of the intense OPO laser beam, we can evaluate the population ratio of the a^4F_J states by considering the transition probabilities of the fluorescence transitions and the LIF signal intensities [5]. We determined the absolute densities of the a^4F_J (J=3/2, 5/2, and 9/2) states from the absolute density of the a^4F_J state and the population ratio.

Figure 9 shows the two-dimensional distributions of the Ti^+ densities at the a^4F_J states. The shapes of the density distributions at the sublevels were almost the same. In contrast to the density distributions of Ti shown in Fig. 6, the peaks of the density distributions of Ti^+ were located at a distance of several centimeters from the target. The difference in the distributions as well as the ratio between the absolute densities of Ti and Ti^+ are helpful information for successful deposition in the narrow trenches and holes, and further discussion will be described in a separate paper.

4. CONCLUSION

The distributions of the absolute Ti and Ti^+ densities were measured successfully by LIF imaging spectroscopy combined with UVAS. The absolute densities of the sublevels of Ti and Ti^+ were evaluated separately, and the total absolute densities were obtained by summing the densities of the sublevels. The absolute densities of Ti and Ti^+ were on the order of 10^{10}~10^{11} and 10^9~10^{10} cm^{-3}, respectively. The absolute densities and the density distributions are helpful information for successive deposition of the barrier layer in narrow trenches and holes.

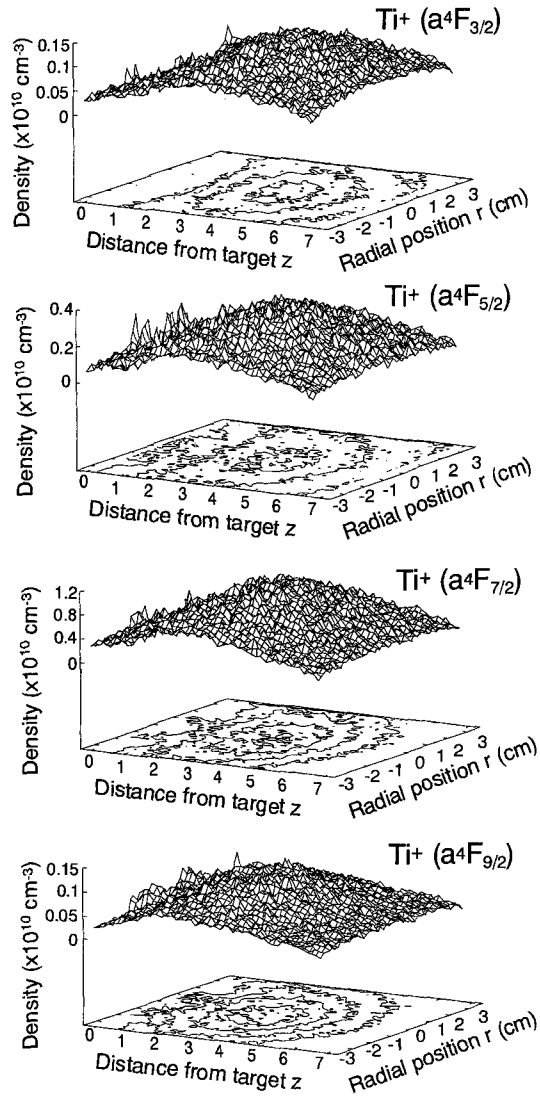

Figure 9. Two-dimensional distributions of the Ti^+ (a^4F_J) densities. The discharge power was 75W and the Ar gas pressure was 100 mTorr.

5. REFERENCES

[1] A. Bogaerts and R. Gijbels, J. Appl. Phys. 72, 1279 (1996).

[2] A. Bogaerts, E. Wagner, B. W. Smith, J. D. Winefordner, D. Pollmann, W. W. Harrison, R. Gijbels, Spectrochimic. Acta Part B 52, 205 (1997).

[3] C. Christou and Z. H. Barber, J. Vac. Sci. Technol. A 18, 2897 (2000).

[4] K. Sasaki, S. Matsui, H. Ito and K. Kadota, J. Appl. Phys. 92, 6471 (2002).

[5] NIST Atomic Database, http://physics.nist.gov/cgi-bin/AtData/main_asd.

[6] A. G. Mitchell and M. W. Zemansky, Resonance Radiation and Excited Atoms (Cambridge University, Cambridge, England, 1961) p. 92.

(Received December 23, 2004; Accepted January 31, 2005)